REVISTA MATÉRIA V.27 N.04
ISSN 1517-7076 articles e20220167, 2022

Temperature and annealing time influences on cross-rolled 7475-T7351 aluminum alloy

Saulo Brinco Diniz[1], Andersan dos Santos Paula[2], Luiz Paulo Brandão[2]

[1]Centro Federal de Educação Tecnológica Celso Suckow da Fonseca, Departamento de Engenharia Metalúrgica, Rua do Areal, n. 522, Parque Mambucaba, Angra dos Reis, RJ, Brasil.

[2]Instituto Militar de Engenharia, Seção de Engenharia de Materiais, Praça General Tibúrcio, n. 80, Urca, Rio de Janeiro, RJ, Brasil.

e-mail: saulo_brinco@hotmail.com, saulo.diniz@cefet-rj.br, andersan@ime.eb.br, brandao@ime.eb.br

ABSTRACT

During production and heat treatments of aluminum alloys, numerous second phase particles form, which maximizes their mechanical properties. This work aimed to perform a correlation between Vickers hardness and X-ray diffraction results, when 7475-T7351 aluminum alloy processed by the cross rolling is subjected to annealing heat treatments (AHT) at 500 ºC for different soaking times (15, 30 and 60 minutes) and for a soaking time of 15 minutes at different temperatures (200, 300 and 400 ºC). The influence of the AHT (500 ºC / 15 minutes) on the microstructure, via scanning and transmission electron microscopy, and tensile tests properties was also investigated. The results show evidence that the Vickers hardness decreased for AHT performed at 200 and 300 ºC / 15 minutes and increase for greater temperatures and times. This behavior is probably due to modifications in the constituent/dispersoid particles and aluminum matrix observed from the X-ray analysis. Partial recrystallization and a coarsening of the precipitates was observed after the AHT at 500 ºC / 60 minutes, whose brought harmful effects on the tensile mechanical properties.

Keywords: 7475-T7351 Aluminum Alloy; Microstructure; Annealing Heat Treatment; Cross Rolling.

1. INTRODUCTION

Aluminum alloys are the most used nonferrous metals worldwide due to their several characteristics and advantages [1, 2]. Among aluminum alloys, the 7XXX series alloys stand out because the possibility to performing aging heat treatments, due their chemical composition, which make possible to obtain a tensile strength near to 600 MPa [3–7]. They are widely used on aircraft components because they align high tensile strength, good ductility, high corrosion resistance, high fatigue strength and low density [3, 4, 6].

The 7475 aluminum alloy has gained prominence among the 7XXX series due to a high mechanical strength and a high tenacity to fracture (up to 52 MPa.$m^{1/2}$) [1, 3, 4, 6]. Its basic chemical composition (in weight %) is 5.2 to 6.2% Zn, 1.90 to 2.6% Mg, 1.2 to 1.9% Cu, 0.18 to 0.25% Cr, who is a modified version of 7075 alloy with a reduction of the maximum content of impurities (Fe + Si) from 0.90% to 0.22% by weight [8, 9].

The 7XXX series aluminum alloys are generally subjected to mechanical and thermal processing routes to maximize a certain characteristic. The T7351 route aims to maximize the corrosion resistance in detriment of the mechanical properties through the alloy overaging [3, 8]. For the 7475 aluminum alloy, the T7351 consists of a solution heat treatment conducted at temperature of 510 °C, [3, 8] a strain relief [4, 9], an aging heat treatment at 107 °C during 6 to 8 hours [3, 8], and finally an overaging heat treatment, which is performed at 163 °C for 24 to 30 hours [3, 8].

There is the formation of "second phase" micro-constituents with the alloy casting and heat treatments on 7XXX series aluminum alloys. They can be divided into three different groups: [3, 4, 7, 10–12] (i) the primary particles (commonly Al_7Cr, Al_3Ti e/ou Al_3Zr) are the first to solidify even before aluminum; (ii) the constituent particles (commonly Al_7Cu_2Fe, $Al_{12}(Fe,Mn)_3Si$, $Al_6(Fe,Mn)$, Mg_2Si, SiO_2, Al_2CuMg and $Al_{23}CuFe_4$), that are usually coherent with the matrix, have a coarse size and can be insoluble or partially soluble; and (iii) the dispersoids (commonly $Al_{12}Mg_2Cr$ and $MgZn_2$) which are commonly smaller than 1 μm.

Generally, heat treatments performed on 7XXX series aluminum alloys have as main objective to promote hardening due to a wide dispersion of dispersoids (usually η' and η) along the matrix [13]. The dispersoid

Corresponding Author: Saulo Brinco Diniz Received on 07/07/2022 Accepted on 29/09/2022

DOI: https://doi.org/10.1590/1517-7076-RMAT-2022-0167

η', which has a chemical formula with different ratios between the Mg and Zn depending on the literature [5, 14], is metastable and coherent with the aluminum matrix. The dispersoid η ($MgZn_2$) is thermodynamically more stable and incoherent with the matrix [1, 5, 14].

The η' dispersoids create stress fields around them, making it difficult to the dislocations slide, or even causing their pinning [14], thus, a larger volumetric fraction of the η' dispersoids, increases the 7XXX series aluminum alloys mechanical strength. [13, 14] Similarly, the 7xxx series alloys mechanical strength decreases, for temperatures above 150 ºC, may be associated with the solubilization of the η' dispersoids leading to the formation of $MgZn_2$ dispersoids, or the coalescing of the η' dispersoid. [13, 14]

In addition to the T7351 treatment, cold forming processes, such as rolling, can also be used to increase the tensile strength of the 7XXX series aluminum alloys [7, 10]. During cold forming processes, important events occur that change the mechanical properties, such as: increase in dislocations density (hardening) and vacancy, change in grain shape which become elongated in the mechanical work direction, and developing crystallographic texture [15–19].

As a disadvantage, cold forming processes reduce the alloy ductility mainly due to hardening, and for this reason, an additional heat treatment step is required to recover the alloy ductility. The heat treatments used for this purpose is the annealing, which has the function of restoring the ductility due to nucleation of stress-free grains that grow and consume the deformed / recovered grains. This results in a new grain structure with a low dislocation density [17, 20–23].

This work aimed to perform a correlation between Vickers hardness and X-ray diffraction results, when a cross-rolled 7475-T7351 aluminum alloy is subjected to annealing heat treatments (AHT) at 500 ºC for different soaking times (15, 30 and 60 minutes), and for a soaking time of 15 minutes at different temperatures (200, 300 and 400 ºC). In addition, it was identified which microstructural modifications occur and their influences on the mechanical properties when the cross-rolled 7475-T7351 aluminum alloy is submitted to AHT at 500 ºC for 1 hour.

2. MATERIAL AND METHODS

2.1. Material

For this study it was used a 7475-T7351 aluminum alloy on hot-rolled slab condition with an initial thickness of 12.5 mm (according to Society of Automotive Engineers, 2012) [24]. Its chemical composition (in weight %) is: 5.67%Zn, 1.78%Cu, 2.38%Mg, 0.2%Cr and 0.28%Fe + Si.

2.2. Methods

The alloy was cross-rolled in a pilot mill FENN MFG. Co., D 51710:1973. For the first, third, fifth and seventh cross-rolling passes, the 7475-T7351 plate was turned 90° angle with relation to its original hot rolling direction. The second, fourth and sixth passes was processed on its hot rolling direction, characterizing the cross-rolling. The rolling passes were performed at room temperature, with a reduction in thickness of about 10% per pass up to thickness of 6.2 mm (called Z sample) [25]. In order to improve the reader's understanding of the cross-rolling processing, Figure 1 shows a schematic figure of how the processing was performed.

The annealing heat treatment (AHT) of the cross-rolled samples was performed in an EDG 3000 furnace. For the annealing performed at 500 ºC, different soaking times were used (15, 30 and 60 minutes, Z5a, Z5b and Z5c samples, respectively) and for a soaking time of 15 minutes the annealing was carried out at different temperatures (200, 300 and 400 ºC, Z2a, Z3a and Z4a samples, respectively).

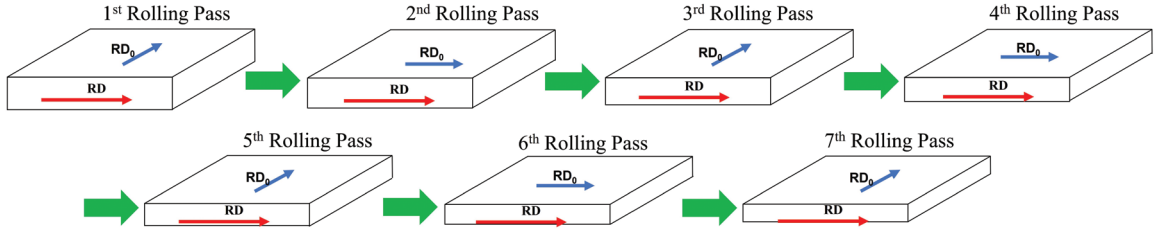

Figure 1: Sequence of passes performed in the present work for cross-rolling.

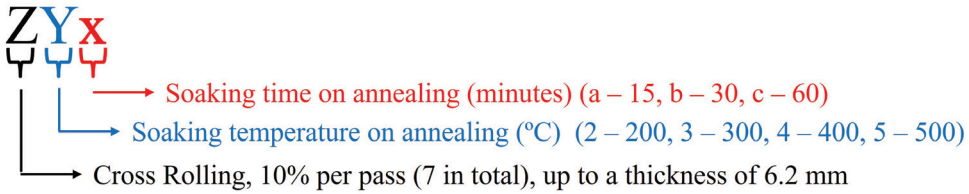

Figure 2: Short nomenclature established for samples in study.

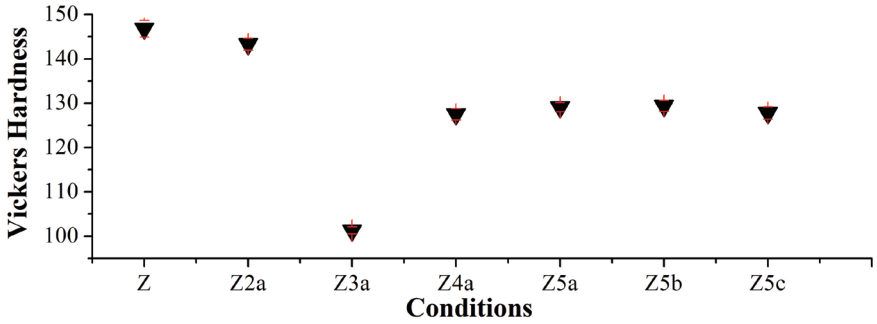

Figure 3: Vickers hardness (mean and standard deviation) variation.

In order to facilitate the discussions, a sample nomenclature was established as exhibited on Figure 2: first letter refers to the start condition after complete cross-rolling (Z) followed by a number that denotes the soaking temperature imposed on annealing (2–200 ºC, 3–300 ºC, 4–400 ºC and 5–500 ºC), and finally the soaking time on annealing (a – 15 minutes, b – 30 minutes and c – 60 minutes).

For all samples, the X-ray diffraction (XRD) and Vickers hardness analysis were performed in the slab plane in a position about ¼ of the thickness. The microstructure analyses were performed by a scanning electron microscope (SEM) in a position about ¼ of the cross-rolled sample thickness (Z and Z5c samples).

Samples for XRD and Vickers hardness analysis were sanded with 220 to 2500 mesh silicon carbide sandpaper, mechanically polished with diamond abrasives (3 μm and 1 μm), and finally electrolytic polishing using a solution of 30% HNO_3 + 70% CH_3OH (% by volume), cooled at –30 ºC, using 10 to 15 volts for 10 to 30 seconds.

The Z and Z5c samples, visualized by SEM FEI Quanta 250 FEG with a voltage of 15 kV, spot size of 4.5 and working distance of 8.0 mm, were additionally etched by KELLER reagent (2.5% HNO_3, 1.5% HCl, 1.0% HF and 95% H_2O) for approximately 50 s.

Ten Vickers hardness measurements were performed at 10 kgf /20 s in an Instron-Wolpert hardness tester for each sample. The X-ray diffractograms were recorded on an X-ray diffractometer PANalytical X'PERT PRO MRD with Co radiation, step size of 0.0394º, time per step of 50 s, and 2θ scan from 3 to 110º. The following JCPDS data were used to identify the diffraction peaks: Al (00-001-1180), Al_2CuMg (03-065-2501), $MgZn_2$ (03-065-3578), $MgSi_2$ (00-017-0081) and Al_7Cu_2Fe (03-065-1685).

Transmission Electron Microscopy (TEM) was carried out on a JEOL JEM-2010 electron microscope. The samples were cut in 3 mm diameter discs using a mechanical punch, sanded to reduce their thicknesses and submitted to an electrolytic polishing by a Struers Tenupol 5, with a solution of 30% HNO_3 + 70% CH_3OH (% by volume).

The uniaxial tensile tests (EMIC DL60000) at room temperature were performed on three samples in Z and Z5c conditions that followed the ASTM E08-M standard [26] for 50 mm gauge length base sample, using a loading speed of 1.0 mm/min. The yield strength (YS) was obtained by a straight line parallel to the elastic line of the stress strain curve offset by 0.2%.

3. RESULTS AND DISCUSSION

3.1. Vickers hardness and x-ray diffraction correlation

Figure 3 shows the mean and standard deviation values of the Vickers hardness measurements of the samples under study. With the AHT temperature rising to 400 ºC (Z4a sample), there was a Vickers hardness increase in

relation to Z3a sample from 101.3 ± 0.8 HV to 127.5 ± 1.3 HV. Increasing the soaking temperature from 400 ºC to 500 ºC (Z4a and Z5a samples, respectively), and for soaking time of 30 and 60 minutes (Z5b and Z5c samples, respectively) the Vickers hardness values kept close with mean values and standard deviations of 127.5 ± 1.3; 129.1 ± 1.0; 129.4 ± 1.3 and 127.8 ± 1.4 HV, respectively. Due to the small hardness variation observed for these samples, it is possible infer that possibly there was no significant changes in the aluminum matrix, in volumetric fraction or "second phase" size and micro-constituents among them.

XRD analyses were performed to understand the aluminum matrix evolution and constituent/dispersoid particles due to the AHT. The diffractograms were divided into two groups: the first group presented in Figure 4 formed by the Z, Z2a, Z3a and Z4a samples, and the second one with the Z5a, Z5b and Z5c samples, which XRD patterns presented in Figure 5. Due to the high peak intensity of the aluminum matrix planes in comparison to

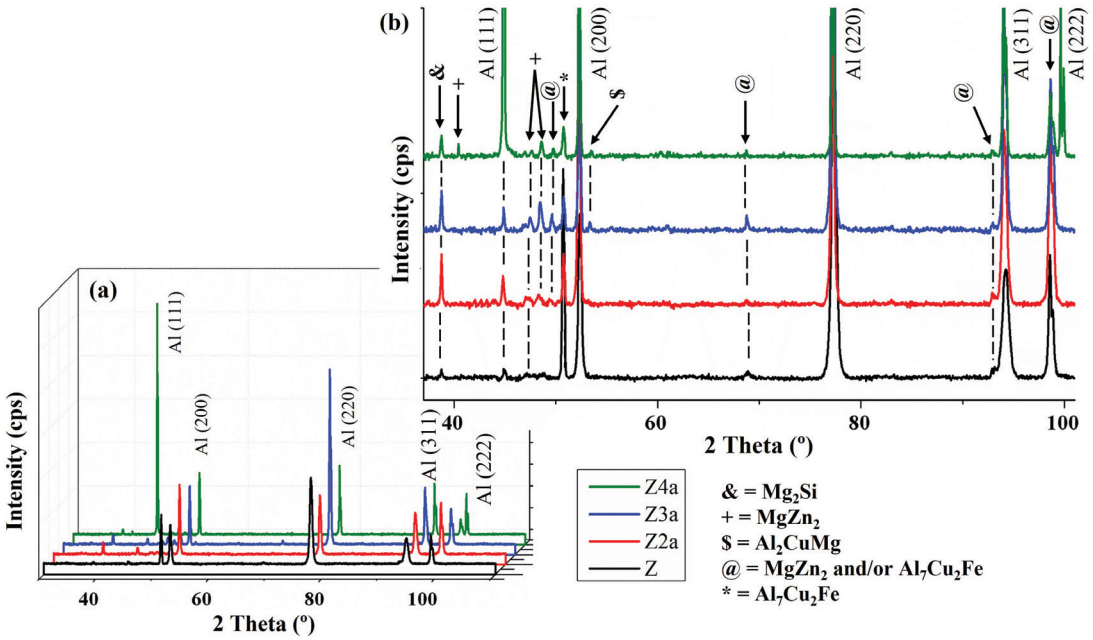

Figure 4: XRD patterns of Z, Z2a, Z3a and Z4a samples. (a) General aspect and (b) highlighting the precipitated peaks.

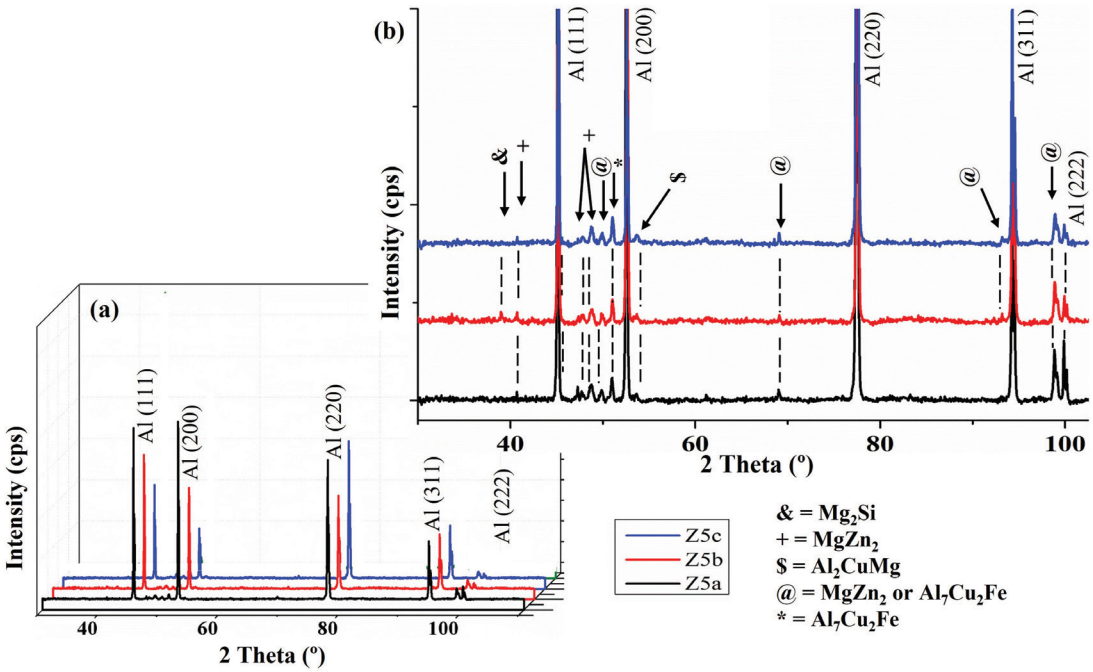

Figure 5: XRD patterns of Z5a, Z5b and Z5c samples. (a) General aspect and (b) highlighting the precipitated peaks.

the constituent/dispersoid particles, the Figures 4b and 5b present a magnification of the region between 38º < 2θ < 101º in order to highlight the particle peaks.

There are many constituent/dispersoid particles of this alloy described in the literature [1, 3, 4, 12, 27–30] with the elements Al-Si-Fe-Zn-Mg-Cu. Therefore, the most frequent phases that are cited as $MgZn_2$, Al_7Cu_2Fe, Al_2CuMg and Mg_2Si were used to identify the possible peaks in the XRD patterns of Figures 4 and 5. Thus, it was possible to identify the aluminum phase and peaks of the following constituent/dispersoid particles: η' and/or $MgZn_2$ (+), Al_7Cu_2Fe (*), Al_2CuMg ($) and Mg_2Si (&). Since the particles peak are very close in the XDR patterns and in order to facilitate their identifications in the Figures 4 and 5, the ones labelled as @ are assigned to Al_7Cu_2Fe or $MgZn_2$ and the others tagged as # are attributed to Al_2CuMg, $MgZn_2$ or Al_7Cu_2Fe. It can be observed in the XDR pattern of sample Z, one high intensity peak at 2θ of 50.50°, which were assigned to Al_7Cu_2Fe particle. As already reported [8, 9], the Fe appears in aluminum alloys as impurity. This high intensity diffraction peak may probably be associated with a relatively high volumetric fraction of the just cited phase in the analyzed region. For Z sample other diffraction peaks indicated by @ were observed, which match the $MgZn_2$ dispersoids or the Al_7Cu_2Fe constituent particles.

The Z2a sample diffractogram presents the aluminum matrix peaks slightly more intense than those of Z sample. This probably indicates that the AHT performed at 200 ºC did not provide significant modifications to the aluminum metal matrix. Comparing the constituent/dispersoid particles diffraction peaks, one can observed that the peak associated with Al_7Cu_2Fe particle located at 2θ of 50.50° has its intensity reduced from Z to Z2a sample. This trend of intensity decreasing is observed until the Z4a sample. After this, the peak intensities keep relatively close until the Z5c sample. That reported decrease of diffraction intensity of the Al_7Cu_2Fe constituent particles may be associated to partial solubilization of them.

It can be also noted a small intensity increase of some diffraction peaks associated with the $MgZn_2$ dispersoids and Mg_2Si constituent particles on the comparison of the X-ray patterns of the Z and Z2a samples. This intensity increase can be correlated with the onset of coalescing of the constituent/dispersoid particles, turning them larger and thus detectable by XRD. Although the small decrease in hardness observed in Figure 3 from the Z to Z2a sample that may be associated with the coalescing of the constituent/dispersoid particles.

With the AHT temperature increase to 300 °C (Z3a sample), the aluminum peak assigned to the plane (220) stand out among the others. This can possible be connected to the beginning of recrystallization. As reported [17] after a large cold rolling deformation the plate or sheet can develop a crystallographic texture. Afterward, during the following heat treatment a recrystallization texture could be evolved. Some authors reported that last texture can be generate by oriented nucleation or oriented growth or even a combination of them. [17, 31, 32] Observing de X ray patterns in Figure 4, it is possible to propose that cited increasing in the intensity of (220) may be associated with preferred nucleating of this orientation in the very beginning of nucleation process, which is consistency with the drop in hardness noted for this sample. One can also note a change in peaks intensity for the sample heat treated at 400 °C (Z4a sample). In this last case the highest peak is the (111) instead of (220). It is coherent with the preferential grow of that orientation as the recrystallization process went on. The same (111) peak is also the one with the highest intensity for the Z5a sample, heat treated at 500 °C, what show consistency with the texture evolution. Summing up, the sample Z3a is probably partially recrystallized and the other two should be fully annealed. The increase in hardness observed for the samples Z4a and Z5a can be debited in the precipitation process occurred concomitant with recrystallization.

In the zoom graphs of the Figures 4 and 5, the diffraction peaks located between the 45 to 50° can be associated with the $MgZn_2$ dispersoids (&) and Al_7Cu_2Fe constituent particles (*). The peaks of the Al_2CuMg constituent particle ($) are at about 53° and the other of $MgZn_2$ dispersoids or Al_7Cu_2Fe constituent particles (@) are around 69°. It can be observing the definition of them with the heat treatments on comparison with the as deformed material, showing the precipitation of dispersoids and constituent particle occurred simultaneously with recrystallization. One can highlight these peaks almost do not exist for Z sample, that they are exceedingly small for Z2 material or are not present and are well define for heat treatments at higher temperature. These results are consistent with the hardness drop noted in Figure 3. On the other hand, the peak precipitations observed in the XRD patterns that was clearly intensified for heat treatment temperature equal or above 400 °C, probably was responsible for the increase the material hardness. The behavior presented by Z5a to Z5c samples are similar with that presented by Z4a. Besides that, one can observe for heat treatment temperature of 500 °C increasing the soaking times for 15, 30 and 60 minutes (Z5a, Z5b and Z5c samples, respectively), no significant modification is observed in the intensities of X ray peaks.

3.2. Microstructural and mechanical characterization of Z and Z5c samples

In order to understand better the microstructural evolution and mechanical properties of the cross-rolled 7475-T7351 aluminum alloy and subsequent annealing, SEM, TEM and uniaxial tensile tests were performed on Z

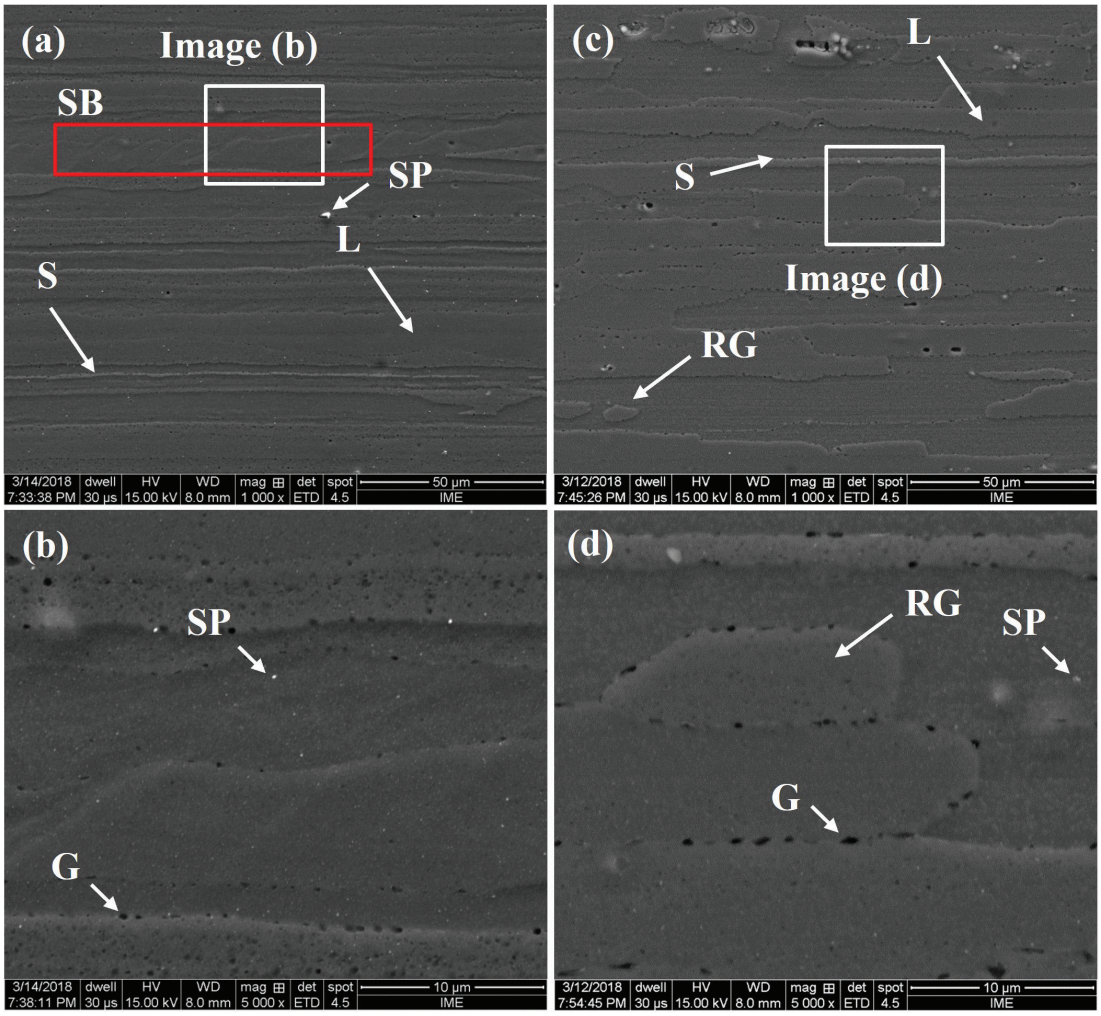

Figure 6: Microstructure of Z ((a) and (b)) and Z5c ((c) and (d)) samples visualized by SEM with lower magnification ((a) and (c)) and higher magnification ((b) and (d)).

and Z5c samples. The Figure 6 shows the microstructures of both samples obtained by SEM with different magnifications: ((a) and (c)) lower magnification and ((b) and (d)) higher magnification. After chemical etching was possible to observe some "pits" on the samples that was assigned by letter "G". One can associate these with the particles release from the matrix due to the action of KELLER reagent. The Z sample (Figures 6a and b) presents elongated grains in its original rolling direction that can be divided in 2 different categories as a function of their thickness: some has a larger and other smaller thickness, identified in the figures by "L" and "S", respectively. It is also observed a substructure, eventually presents in cold deformed materials with high stacking fault energy, in one grain that is indicated by "SB" in the Figure 6b of Z sample.

In Z5c sample (Figures 6c and d) there is evidence of the occurrence recrystallisation associate with different grain morphologies (assigned as RG) after AHT compared to the deformed sample. However, the presence of grains with elongated formats is observed both with a larger (indicated by "L") and smaller (indicated by "S") thickness. This indicates that the Z5c sample was possibly not complete recrystallized or else the contrast offered by the SEM/sample preparation route was not effective to reveal all the grain boundaries.

In Figure 7 it is possible to observe the microstructures of the Z and Z5c samples obtained by TEM analysis. Figures ((a) and (b)) are acquired with lower and ((c) and (d)) for higher magnifications. According to these Figures, one can observe that Z sample presents elongated grains, designated by "EG", parallel to its original rolling direction. It is not possible to accurately differentiate the grain that has a smaller and larger thickness probably due to small observed region peculiar of TEM technique.

On the comparison of the microstructures of Z and Z5c samples, one can highlight that Z sample presents coarse and elongated grains while Z5c sample shows a microstructure formed by a mixture of recrystallized

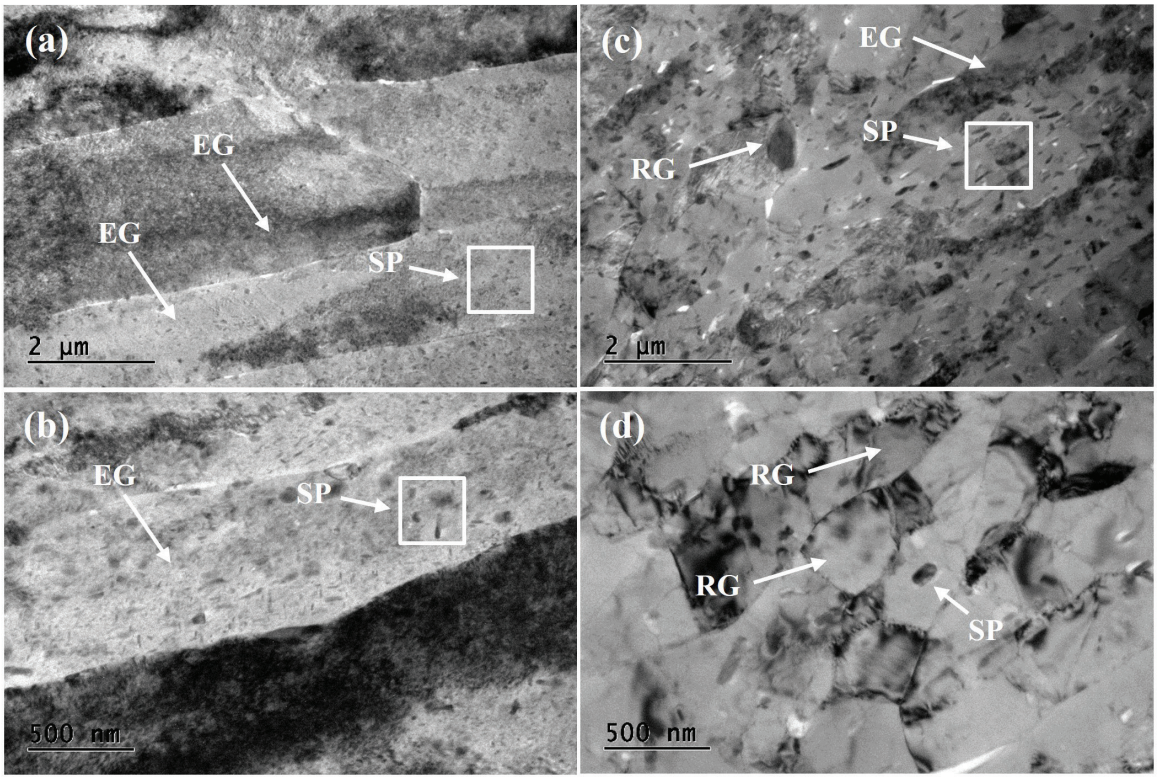

Figure 7: Microstructure of Z ((a) and (b)) and Z5c ((c) and (d)) samples visualized by TEM with lower ((a) and (c)) and higher ((b) and (d)) magnification.

grains and elongated grains nominated in the figures by "RG" and "EG", respectively. It can be possible to observe some coarse and elongated grains for Z5c material in Figures 6 and 7. So, it can be drawn out that the AHT performed at 500 ºC for 1 hour was not enough to completely recrystallized the Z sample.

The 7XXX series alloys have a large amount of second phase micro-constituents. Because of it, the recrystallized grains usually have a large range of sizes. LIAO *et al.* [28] studied the influence of different Cu percentage in %weight in the recrystallization kinetics of 7XXX series aluminum alloy. They concluded that higher the Cu content higher is the volumetric fraction of second phase micro-constituents, which strongly influence the alloy recrystallization kinetics and, consequently, its final microstructure. It can be also observed in the TEM images the increase of the second phase micro-constituent particle sizes, indicated by "SP" in the Figures 6 and 7. This was probably due to the coalescing of the smaller particles during the AHT. This is consistent with the results of X-ray diffraction, Figures 4 and 5, previously presented.

The uniaxial tensile test was performed to find out the influence of AHT on the properties of the yield strength (YS), ultimate tensile strength (TS) and the uniform strain (ε). In the Figure 8a are presented the engineering stress-strain curves of three Z sample specimens and two Z5c sample specimens. The table in Figure 8b shows the average and standard deviations values of the yield strength (YS), ultimate tensile strength (TS) and the uniform strain (ε) obtained for Z and Z5c samples. For Z sample the mean values and standard deviations for ε, YS and TS were 7.7 ± 1.0%, 458.1 ± 11.0 MPa and 481.1 ± 9.9 MPa, respectively. For the Z5c specimens these values were 16.7 ± 0.3%, 186.0 ± 9.5 MPa and 371.9 ± 8.2 MPa, respectively.

According to SAE AMS 4202 standard [13] the minimum mechanical properties for 7475-T7351 aluminum alloy in the plate (thickness between 6.35 and 38.1 mm) form should be 414 MPa for YS, 490 MPa for TS and 10% of deformation, respectively. Comparing these values with those obtained for Z sample (rough state), it can be observed that the values obtained for TS and ε are slightly lower than the minimum values established by standard SAE AMS 4202 [13]. On other hand, YS values are higher than the minimum settled by the standard.

KADLEC *et al.* [33] also carried out tensile tests rolled sheet of 7475-T7351 aluminum alloy and obtained 429.9 ± 0.8 MPa, 502.2 ± 0.7 MPa and 16.5 ± 0.6% for YS, TS and ε, respectively. These values are consistent with the SAE AMS 4202 standard [13]. According to the authors, the average grain size of the tested

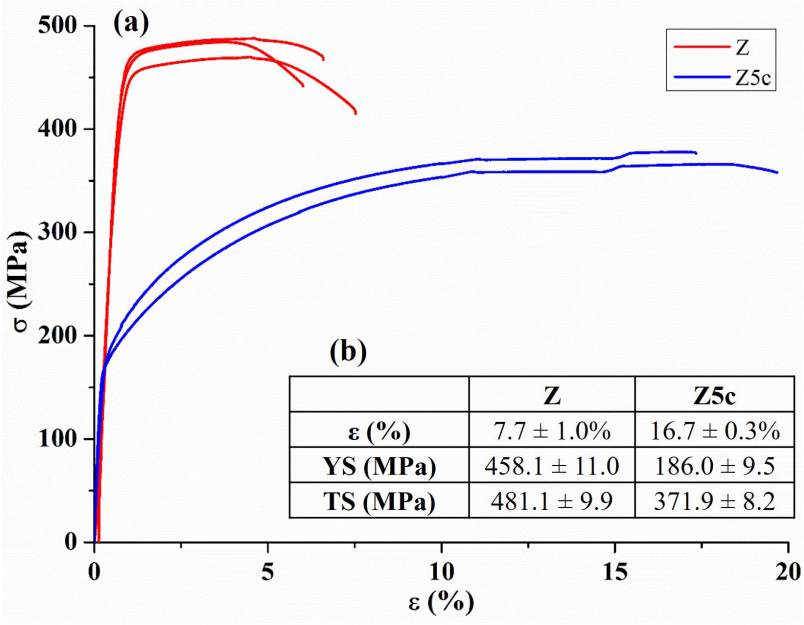

	Z	Z5c
ε (%)	7.7 ± 1.0%	16.7 ± 0.3%
YS (MPa)	458.1 ± 11.0	186.0 ± 9.5
TS (MPa)	481.1 ± 9.9	371.9 ± 8.2

Figure 8: (a) Engineering Stress – Strain curves (σ (MPa) x ε (%)) for Z and Z5c samples. (b) Average and standard deviations values of YS, TS and ε.

material was of 30.1 and 9.4 μm, for the longitudinal and transversal rolling direction, respectively. One of the possible reasons for the poor mechanical properties values obtained in our investigation may be associated with the coarse grain structure elongated in the rolling direction as observed in the SEM images, Figure 6.

The YS and TS values obtained for the Z5c sample are even lower than those noted for Z sample. Consequently, they are 24 and 55% lower than the minimum values stipulated by the SAE AMS 4202 standard [13], respectively. However, there was an increase of 60% in the value of ε, in relation to the minimum stipulated by the SAE AMS 4202 standard [13].

Based on the presented results, it is concluded that the AHT using high temperatures and long times can be harmful for the tensile properties of the 7475-T7351 aluminum alloy. Consequently, the grain structure obtained in this investigation is not indicated for conformation of parts where high temperatures and long times are used.

4. CONCLUSIONS

- A decrease in the Vickers hardness was observed until the annealing heat treatment performed until 300 ºC. This fact may be associated with the coalescing of the constituent/dispersoid particles and start of the recrystallization process. It was observed an increased in hardness observed after the annealing heat treatment performed at 400 ºC, which can be associated with the precipitation process occurred concomitant with recrystallization. For higher temperatures and soaking times (500 ºC, and times of 15 to 60 minutes), there was an increase in the hardness, but without a significant variation between them;
- The cross-rolled sample shows an elongated and coarse grains microstructure oriented in the original rolling direction. After an annealing heat treatment 500 ºC for 60 minutes, observed at least a partial recrystallization with some elongated coarse grains present in the microstructure;
- The cross-rolled sample shows yield strength, ultimate tensile strength and ductility close to the minimum values established by the SAE AMS 4202 standard, but after the annealing heat treatment at 500 ºC / 60 minutes, there was a drastic reduction in these properties.

5. ACKNOWLEDGMENTS

The authors thank CAPES for a PhD scholarship (2014-2017 / DINIZ, S.B.); the Universidade Federal Fluminense (UFF), for the tensile tests; Centro Federal de Educação Tecnológica Celso Suckow da Fonseca (CEFET/RJ - Maracanã) for the use of the Instron Wolpert durometer; Universidade Federal do Rio de Janeiro (UFRJ / COPPE), for preparing the samples for TEM; Eletron Microscopy Laboratory of the Instituto Militar de Engenharia (LME/IME), for use SEM and TEM equipaments.

6. BIBLIOGRAPHY

[1] ZHANG, X., CHEN, Y., HU, J., "Recent advances in the development of aerospace materials", *Progress in Aerospace Sciences*, v. 97, pp. 22–34, 2018. doi: http://dx.doi.org/10.1016/j.paerosci.2018.01.001.

[2] ASM INTERNATIONAL, *Properties and Selection: Nonferrous Alloys and Special-Purpose Materials*, vol. 2, Materials Park, 1990.

[3] BRAGA, A.P.V., "*Análise de ligas de alumínio aeronáuticas conformadas por jateamento com granalhas: caracterização e previsão de deformação*", Tese de M.Sc., Universidade de São Paulo, São Paulo, 2011.

[4] ROMETSCH, P.A., ZHANG, Y., KNIGHT, S., "Heat treatment of 7xxx series aluminium alloys - some recent developments", *Transactions of Nonferrous Metals Society of China*, v. 24, n. 7, pp. 2003–2017, 2014. doi: http://dx.doi.org/10.1016/S1003-6326(14)63306-9.

[5] HADJADJ, L., AMIRA, R., "The effect of cu addition on the precipitation and redissolution in Al–Zn–Mg alloy by the differential dilatometry", *Journal of Alloys and Compounds*, v. 484, n. 1-2, pp. 891–895, 2009. doi: http://dx.doi.org/10.1016/j.jallcom.2009.05.082.

[6] DURSUN, T., SOUTIS, C., "Recent developments in advanced aircraft aluminium alloys", *Materials & Design*, v. 56, pp. 862–871, 2014. doi: http://dx.doi.org/10.1016/j.matdes.2013.12.002.

[7] DINIZ, S.B., PAULA, A.S., BRANDÃO, L.P.M., "Structural characterization of the rolled and annealed 7475 aluminium alloy", *Journal of Materials Engineering and Performance*, Jul. 2022. doi: http://dx.doi.org/10.1007/s11665-022-07120-9.

[8] ASM INTERNATIONAL, *ASM Handbook*, vol. 4, Materials Park, 1991.

[9] SOCIETY OF AUTOMOTIVE ENGINEERS, *AMS 2355 Quality Assurance, Sampling and Testing, Aluminum Alloys and Magnesium Alloys, Wrought Products (Except Forging Stock), and Rolled, Forged, or Flash Welded Rings*, Pensilvania, SAE International, 2017.

[10] SOUZA, C.A.C., PAULA, A.S., BRANDÃO, L.P.M., *et al*., "Microstructure and mechanical properties evaluation after annealing heat treatment of 7475-t7351 alluminum alloy", *Brazilian Journal of Development*, v. 8, n. 8, pp. 55772–55785, Aug. 2022. doi: http://dx.doi.org/10.34117/bjdv8n8-072.

[11] TOTTEN, G.E., MACKENZIE, D.S., *Handbook of Aluminum: Physical Metallurgy and Processes*, New York, CRC Press, 2003.

[12] ASM INTERNATIONAL, *Metallography and Microstructures*, vol. 9, Materials Park, 2004.

[13] LEO, P., CERRI, E., MCQUEEN, H.J., *et al*., "Microstructure and mechanical characterization of an Al-Zn-Mg alloy after various heat treatments and room temperature deformation", *Materials Science Forum*, v. 604-605, pp. 67–76, 2009. doi: http://dx.doi.org/10.4028/www.scientific.net/MSF.604-605.67.

[14] YAMAMOTO, A., MINAMI, K., ISHIHARA, U., *et al*., "Calorimetric and resistivity study of formation and redissolution of precipitates in 7050 aluminium alloy", *Materials Transactions*, v. 39, n. 1, pp. 69–74, 1998. doi: http://dx.doi.org/10.2320/matertrans1989.39.69.

[15] SOUSA, T.G., DINIZ, S.B., PINTO, A.L., *et al*., "Dislocation density by x-ray diffraction in α brass deformed by rolling and ECAE", *Materials Research*, v. 18, pp. 246–249, 2015. doi: http://dx.doi.org/10.1590/1516-1439.369214.

[16] PADILHA, A.F., SICILIANO JUNIOR, F., *Encruamento, Recristalização, Crescimento de Grão e Textura*, São Paulo, ABM Livros, 2005.

[17] HUMPHREYS, F.J., HATHERLY, M., *Recrystallization and Relates Annealing Phenomena*, Oxford, Pergamon Editora, 2004.

[18] CASANOVA, A.M.B., DINIZ, S.B., SILVA, C.S., *et al*., "Avaliação da homogeneidade estrutural em liga de alumínio 7475-T7351 submetida a laminação convencional e assimétrica", *Tecnologica em Metalurgia, Materiais e Mineração*, v. 15, n. 3, pp. 202–206, 2018. doi: http://dx.doi.org/10.4322/2176-1523.1572.

[19] VALE, M.G., MEDEIROS, N., FONSECA, G.S., *et al*., "On the mechanical behavior of an Al 7075 alloy deformed by asymmetrical and conventional rolling", *Matéria*, v. 24, n. 1, e-12288, 2019. doi: http://dx.doi.org/10.1590/s1517-707620190001.0625.

[20] SOUZA, C.A.C., DINIZ, S.B., SILVA, A.S., *et al*., "Pre and post-welding annealing influence on the microstructure of a 7475-T7351 aluminum alloy joining by friction stir welding", *Brazilian Journal of Development*, v. 8, n. 2, pp. 15101–15114, Feb. 2022.

[21] SLÁMOVÁ, M., OCENÁSEK, V., VANDER VOORT, G., "Polarized Light Microscopy: Utilization in the investigation of the recrystallization of aluminum alloys", *Materials Characterization*, v. 52, n. 3, pp. 165–177, 2004. doi: http://dx.doi.org/10.1016/j.matchar.2003.10.010.

[22] KIM, J.-K., JEE, Y.-K., HUH, M.-Y., *et al*., "Formation of textures and microstructures in asymmetrically cold rolled and subsequently annealed aluminum alloy 1100 sheets", *Journal of Materials Science*, v. 39, n. 16/17, pp. 5365–5369, 2004. doi: http://dx.doi.org/10.1023/B:JMSC.0000039246.72708.0a.

[23] DINIZ, S.B., BENATTI, E.A., PAULA, A.S., *et al*., "Microstructural evaluation of an asymmetrically rolled and recrystallized 3105 aluminum alloy", *Journal of Materials Research and Technology*, v. 5, n. 2, pp. 183–189, 2016. doi: http://dx.doi.org/10.1016/j.jmrt.2016.02.001.

[24] SOCIETY OF AUTOMOTIVE ENGINEERS, *AMS 4202: Aluminum Alloy Plate 5.7Zn - 2.2Mg - 1.6Cu - 0.22Cr (7475-T7351) Solution Heat Treated, Stress Relieved by Stretching, and Precipitation Heat Treated*, Pensilvania, SAE International, 2012.

[25] DINIZ, S.B., CRUZ, R.B., PAULA, A.S., *et al*., "Evolução microestrutural de uma liga de alumínio 7475-T7351 submetida a laminação cruzada e recristalizada com diferentes tempos de encharque", In: *Anais do 72º Congresso Anual da ABM*, pp. 2119–2129, Rio de Janeiro, 2018.

[26] AMERICAN SOCIETY FOR TESTING AND MATERIALS, *ASTM E8/E8M-16ae1 Standard Test Methods for Tension Testing of Metallic Materials*, West Conshohocken, 2016.

[27] TOTTEN, G.E., MACKENZIE, D.S., *Handbook of Aluminum: Physical Metallurgy and Processes*, New York, Marcel Dekker, 2003.

[28] LIAO, Y.G., HAN, X.Q., ZENG, M.X., *et al*., "Influence of Cu on microstructure and tensile properties of 7XXX series aluminum alloy", *Materials & Design*, v. 66, pp. 581–586, 2015. doi: http://dx.doi.org/10.1016/j.matdes.2014.05.003.

[29] SOUZA, S.H., PADILHA, A.F., "Recozimento da liga de alumínio AA 7075 após laminação a frio", In: *Anais do 72º Congresso Anual da ABM*, pp. 172-182, Rio de Janeiro, 2018. doi: http://dx.doi.org/10.5151/1516-392X-30121.

[30] HUANG, L., LIU, S., DU, Y., *et al*., "Thermal conductivity of the Mg–Al–Zn alloys: experimental measurement and calphad modeling", *Calphad*, v. 62, pp. 99–108, 2018. doi: http://dx.doi.org/10.1016/j.calphad.2018.05.011.

[31] CULLITY, B., STOCK, S.R., *Elements of X-Ray Diffraction*, Massachusetts, Addison Wesley Metallurgy Series, 1956.

[32] LADD, M., PALMER, R., *Structure Determination by X-Ray Crystallography, Analysis by X-Rays and Neutrons*, New York, Springer, 2013.

[33] KADLEC, M., RUZEK, R., NOVAKOVA, L., "Mechanical behaviour of AA 7475 friction stir welds with the kissing bond defect", *International Journal of Fatigue*, v. 74, pp. 7–19, 2015. doi: http://dx.doi.org/10.1016/j.ijfatigue.2014.12.011.